International Journal of Electrical and Power Engineering 5 (2): 92-101, 2011
ISSN: 1990-7958

Modeling and Simulation of a Self-Excited Induction Generator/Inductive Load System

Ibrahim A.M. Abdel-Halim, Hamed G. Hamed and Ahmed M. Hassan
Department of Electrical Engineering, Faculty of Engineering,
Benha University, 108 Shoubra St., Cairo, Egypt

Abstract: In this study, complete Matlab/Simulink block diagrams are constructed to obtain the steady-state performance of a self-excited induction generator, using loop impedance method, using the exact and a previously obtained simplified method to obtain the operating frequency of the generator when feeding inductive loads. The results obtained by the presented approach for the frequency and performance characteristics of the system are compared with results obtained from a published reference to prove the validity of the simulation process.

Key words: Matlab/Simulink, self-excited induction generator, static inductive load, cost, loop, Egypt

INTRODUCTION

The squirrel-cage induction generators which may be operated as Self-excited Induction Generators (SEIG) are good choice for stand alone Wind Energy Conversion System (WECS) because of several advantages such as low capital and maintenance cost, rugged construction, better transient performance and when used as self-excited generators they do not require any external supply to produce excitation magnetic field (Baroudi *et al*., 2007; Nesba *et al*., 2006; Seyoum *et al*., 2003; Wang and Su, 1999). They are also self protected against short circuit because their output voltage collapses when short circuit between their terminals occurs (Nesba *et al*., 2006; Seyoum *et al*., 2003).

In this study, complete Matlab/Simulink block diagrams are constructed to obtain the steady-state performance of the SEIG, using the loop impedance method (Chan, 1994), using the exact and a previously obtained simplified method (Abdel-Halim *et al*., 1999) to obtain the operating frequency of the generator when feeding inductive loads. The obtained results are compared with results obtained from a published reference (Chan, 1994).

MATERIALS AND METHODS

At the steady-state, the values of per-unit operating frequency, a and the magnetizing reactance, X_m for given machine parameters, speed, excitation capacitance and load impedance are obtained (Abdel-Halim *et al*., 1999; Chan, 1994). Upon obtaining the values of a and X_m the steady-state performance of the SEIG can be obtained (Abdel-Halim *et al*., 1999; Chan, 1994).

The steady-state analysis of the SEIG is based on its per-phase equivalent circuit. There are two methods used to obtain the values of a and X_m. These two methods are loop impedance and nodal admittance methods (Chan, 1994). The loop impedance method will be used in this study to obtain the steady-state performance of the SEIG.

The per-phase equivalent circuit of a three-phase SEIG is shown in Fig. 1 (Abdel-Halim *et al*., 1999; Chan, 1994) in which the parameters are referred to rated frequency and are assumed to be independent of saturation except the magnetizing reactance and the core losses and effect of harmonics are neglected (Abdel-Halim *et al*., 1999). Applying Kirchhoff's voltage law on loop (abdca) of Fig. 1 shows:

$$I_1(Z_{ab} + Z_{ac} + Z_{cd}) = 0 \quad (1)$$

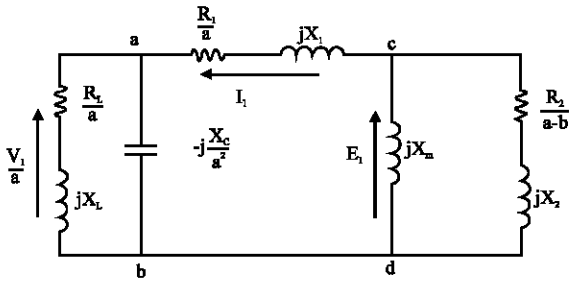

Fig. 1: Per-phase equivalent circuit of SEIG

Corresponding Author: Ibrahim A.M. Abdel-Halim, Department of Electrical Engineering, Faculty of Engineering, Benha University, 108 Shoubra St., Cairo, Egypt

Where:

$$Z_{ab} = \frac{(R_L/a + jX_L)(-jX_c/a^2)}{R_L/a - j(X_c/a^2 - X_L)} \quad (2)$$

$$Z_{ac} = R_1/a + jX_1 \quad (3)$$

$$Z_{cd} = \frac{jX_m(R_2/(a-b) + jX_2)}{R_2/(a-b) + j(X_m + X_2)} \quad (4)$$

Since for successful voltage build up, $I_1 \neq 0$, hence from Eq. 1 (Chan, 1994):

$$Z_{ab} + Z_{ac} + Z_{cd} = 0 \quad (5)$$

Substituting Eq. 2-4 into Eq. 5 gives:

$$\begin{aligned}&[\frac{X_cX_LR_2}{a^2(a-b)} + X_cR_L(X_m + X_2)/a^3 + \frac{R_1R_2R_L}{a^2(a-b)} + \\ &\frac{X_1R_2(X_c/a^2 - X_L)}{(a-b)} - \frac{R_LX_1}{a}(X_m + X_2) + \frac{R_1}{a} \\ &(X_c/a^2 - X_L)(X_m + X_2) - \frac{X_mX_2R_L}{a} + \\ &\frac{X_mR_2(X_c/a^2X_L}{(a-b)}] + j[\frac{X_cX_L(X_m + X_2)}{a^2} - \\ &\frac{R_2X_cR_L}{a^3(a-b)} + \frac{R_1R_L}{a^2}(X_m + X_2) + X_1(X_c/a^2 - X_L) \\ &(X_m + X_2) + \frac{R_LX_1R_2}{a(a-b)} - \frac{R_1R_2}{a(a-b)}(X_c/a^2 - X_L) + \\ &\frac{R_LX_mR_2}{a(a-b)} + X_mX_2(X_c/a^2 - X_L)] = 0\end{aligned} \quad (6)$$

Equating the real part of Eq. 6 to zero yields (Chan, 1994):

$$\begin{aligned}&-(A_1X_m + A_2)a^3 + (A_3X_m + A_4)a^2 + \\ &(A_5X_m + A_6)a - (A_7X_m + A_8) = 0\end{aligned} \quad (7)$$

The coefficients A_{1-8} are given in the Appendix. Equating the imaginary part of Eq. 6 to zero yields (Chan, 1994):

$$\begin{aligned}&-(B_1X_m + B_2)a^4 + (B_3X_m + B_4)a^3 + \\ &(B_5X_m + B_6)a^2 - (B_7X_m + B_8)a - B_{10} = 0\end{aligned} \quad (8)$$

The coefficients B_{1-10} are given in the Appendix. Equation 7 and 8 can be rewritten, respectively as follows (Chan, 1994):

$$X_m = \frac{A_2a^3 - A_4a^2 - A_6a + A_8}{-A_1a^3 + A_3a^2 + A_5a - A_7} \quad (9)$$

$$X_m = \frac{B_2a^4 - B_4a^3 - B_6a^2 + B_8a + B_{10}}{-B_1a^4 + B_3a^3 + B_5a^2 - B_7a} \quad (10)$$

Equation 9 and 10 gives the following 7th degree polynomial in the per-unit frequency, a (Chan, 1994):

$$\begin{aligned}&P_7a^7 + P_6a^6 + P_5a^5 + P_4a^4 + P_3a^3 + \\ &P_2a^2 + P_1a + P_0 = 0\end{aligned} \quad (11)$$

The coefficients P_{0-7} are given in the Appendix. For certain operating per unit speed, b and machine and load parameters, Eq. 11 can be solved numerically using numerical methods such as Newton-Raphson method to obtain the per-unit frequency, a. The value of the per-unit frequency is used either in Eq. 9 or 10 to get the corresponding value of the magnetizing reactance, X_m. The value of the magnetizing reactance and the magnetization curve of the machine are used to obtain the air gap voltage E_1.

Consequently, the equivalent circuit of Fig. 1 can be used to obtain the steady-state performance of the SEIG for an operating speed and load parameters. The magnetizing current, I_m can be obtained from:

$$I_m = \frac{E_1}{Z_m} \quad (12)$$

where, $Z_m = jX_m$ and the rotor current, I_2 can be obtained from:

$$I_2 = \frac{E_1}{Z_2} \quad (13)$$

where, $Z_2 = R_2/(a-b) + jX_m$ and the stator current, I_1 is obtained from:

$$I_1 = \frac{E_1(Z_2 + Z_m)}{Z_2Z_m} \quad (14)$$

The load current, I_L can be obtained from:

$$I_L = I_1\frac{Z_c}{Z_c + Z_L} \quad (15)$$

where, $Z_c = -jX_c/a^2$ and $Z_L = R_L/a + jX_L$ and the load voltage can thus be obtained from:

$$V_L = aI_L Z_L \quad (16)$$

Simulation of the SEIG at steady-state: The SEIG is simulated using Matlab/Simulink software package.

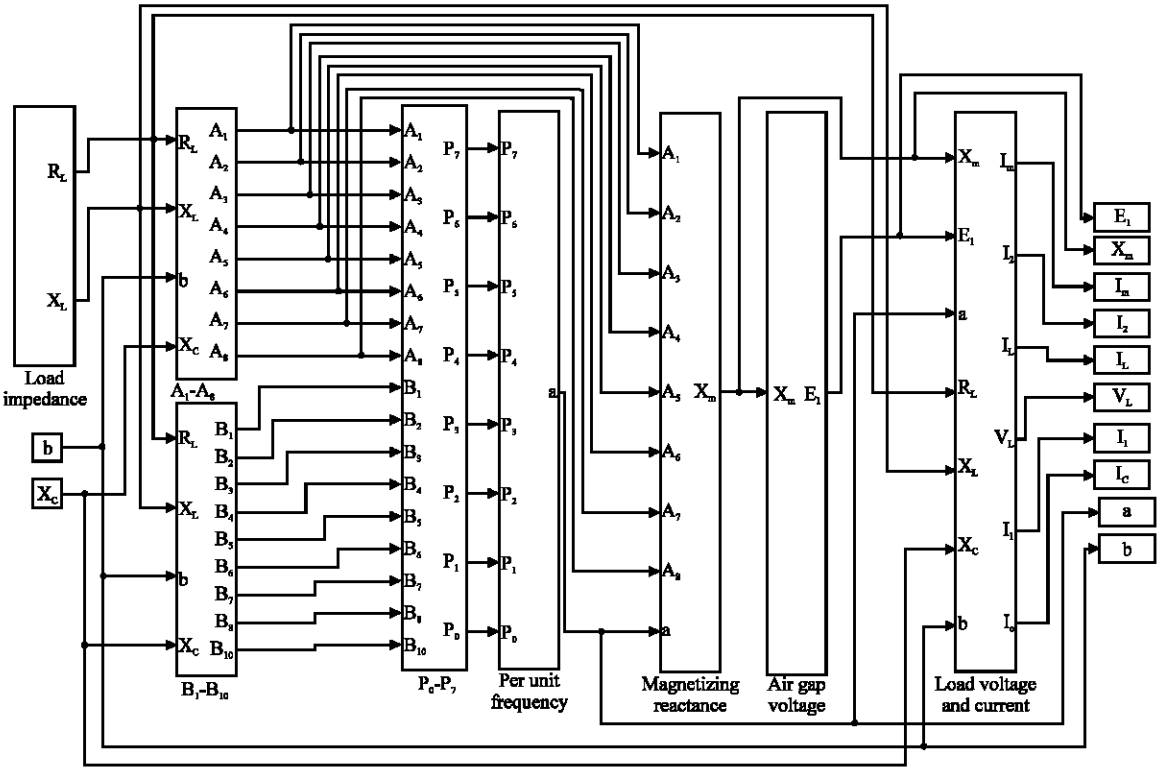

Fig. 2: Overall Simulink block diagram of the SEIG at steady-state

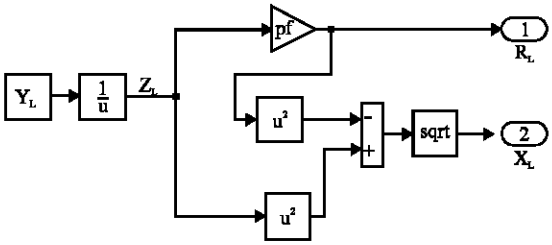

Fig. 3: The subsystem; load impedance

Figure 2 shows the overall Simulink block diagram which consists of several subsystems. The details of the subsystem load impedance are shown in Fig. 3. It is used to obtain the load resistance, R_L and reactance, X_L when the load admittance, Y_L and power factor pf are known. Thus, it represents the following equations:

$$R_L = \frac{pf}{Y_L},\ X_L = \sqrt{\left(\frac{1}{YL}\right)^2 - R_L^{\ 2}} \qquad (17)$$

The obtained load resistance, load reactance and the per unit speed, b are used as inputs to the subsystem A_{1-8} whose details are shown in Fig. 4 to obtain the coefficients A_{1-8} which are given in the Appendix. The coefficients B_{1-10} which given in the Appendix are

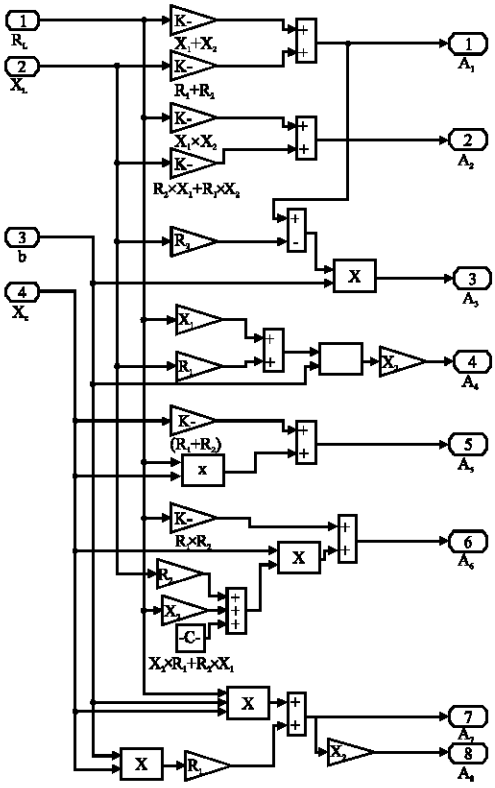

Fig. 4: The subsystem, A_1-A_8

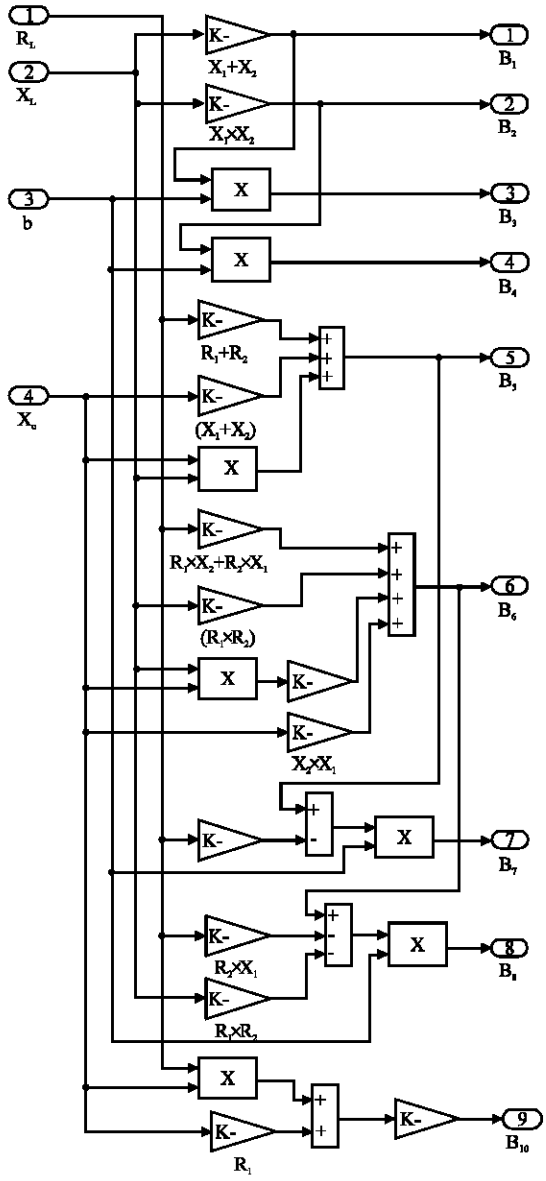

Fig. 5: The subsystem; B_1-B_{10}

obtained from the subsystem $B_{1\text{-}10}$ whose inputs are the load resistance, load reactance and per unit speed. The details of the subsystem $B_{1\text{-}10}$ are shown in Fig. 5. The outputs of the subsystems $A_{1\text{-}8}$ and $B_{1\text{-}10}$ are used as inputs to the subsystem $P_{0\text{-}7}$ to obtain the coefficients $P_{0\text{-}7}$ which given in the Appendix. The details of the subsystem $P_{0\text{-}7}$ are shown in Fig. 6. The outputs of the subsystem $P_{0\text{-}7}$ are used as inputs to the subsystem, per unit frequency whose details are shown in Fig. 7 to obtain the per unit frequency, a. This subsystem represents Eq. 11.

The outputs of the subsystems $A_{1\text{-}8}$ and per unit frequency are used as inputs to the subsystem magnetizing reactance which represents Eq. 9 to obtain the value of X_m. Figure 8 shows the details of the subsystem magnetizing reactance. The obtained value of X_m is used as input to the subsystem air gap voltage to obtain the value of E_1.

This subsystem represents the magnetization curve of the induction machine which is given in the Appendix. The details of the subsystem Air gap voltage are shown in Fig. 9.

The obtained values of E_1, X_m, a, R_L and X_L and the value of the per unit speed, b are used as inputs to the subsystem, load voltage and current whose details are shown in Fig. 10 to obtain the load current, I_L and load voltage, V_L. This subsystem represents Eq. 12-16.

Simplified simulation of the SEIG at steady-state: In this study, a simplified method given in reference (Abdel-Halim *et al*., 1999) by which the per-unit frequency can be obtained directly for given machine parameters, speed, excitation capacitance and a static inductive load without using of the 7th order equation, Eq. 11 is used in the simulation of the SEIG at steady-state. This method (Abdel-Halim *et al*., 1999) depends on that the difference between the per-unit frequency and per unit speed is small. If this difference is denoted by ε then:

$$\varepsilon = a-b \tag{18}$$

Thus, the per unit frequency in Eq. 11 can be substituted by:

$$a = \varepsilon + b \tag{19}$$

Therefore, Eq. 11 can be rewritten as follows:

$$\begin{aligned} &P_7(\varepsilon+b)^7 + P_6(\varepsilon+b)^6 + P_5(\varepsilon+b)^5 + \\ &P_4(\varepsilon+b)^4 + P_3(\varepsilon+b)^3 + P_2(\varepsilon+b)^2 + \\ &P_1(\varepsilon+b) + P_0 = 0 \end{aligned} \tag{20}$$

Since, the value of ε is significantly small, hence the values of ε^n with n>2 can be neglected in Eq. 20. Thus, Eq. 20 can be reduced to:

$$k_2\varepsilon^2 + k_1\varepsilon + k_0 = 0 \tag{21}$$

Where:

$$\begin{aligned} k_2 = {} & 21b^5P_7 + 15b^4P_6 + 10b^3P_5 + \\ & 6b^2P_4 + 3bP_3 + P_2 \end{aligned} \tag{22}$$

$$\begin{aligned} k_1 = {} & 7b^6P_7 + 6b^5P_6 + 5b^4P_5 + \\ & 4b^3P_4 + 3b^2P_3 + 2bP_2 + P_1 \end{aligned} \tag{23}$$

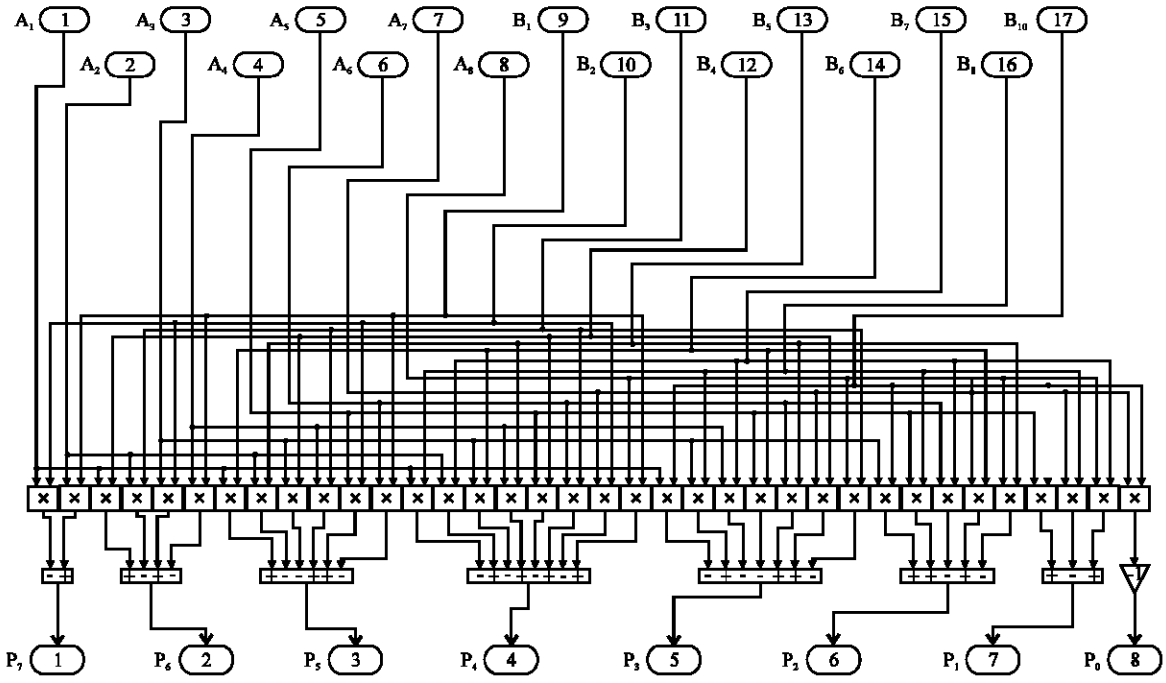

Fig. 6: The subsystem; P_0-P_7

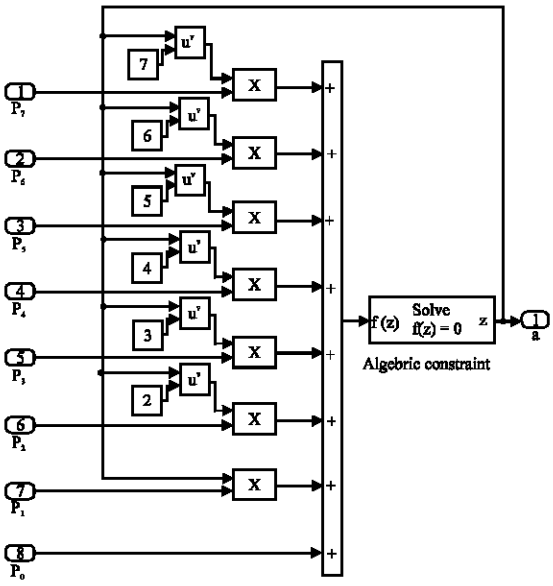

Fig. 7: The subsystem, per unit frequency when the loop impedance method is used

$$k_0 = b^7P_7 + b^6P_6 + b^5P_5 + b^4P_4 + b^3P_3 + b^2P_2 + bP_1 + P_0 \quad (24)$$

It can be noticed that Eq. 21 is a 2nd order equation which is simpler to be solved than Eq. 11 which requires numerical solution. The per unit frequency can thus be obtained directly using Eq. 21 from:

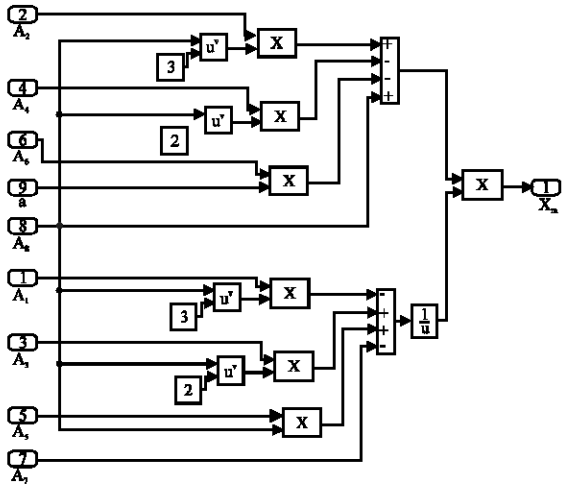

Fig. 8: The subsystem, magnetizing reactance

$$a = b - \frac{k_1 - \sqrt{k_1^2 - 4k_0k_2}}{2k_2} \quad (25)$$

The obtained per unit frequency is used to obtain the magnetizing reactance from either Eq. 9 or 10. The equations of the performance of the SEIG given in Eq. 3 can thus be used.

The Matlab/Simulink simulation of the generator in this case can be obtained as shown in Fig. 11. Figure 11 consists of several subsystems. All of these subsystems were explained in the previous study

except that the details of the subsystem, per unit frequency are changed to be as shown in Fig. 12.

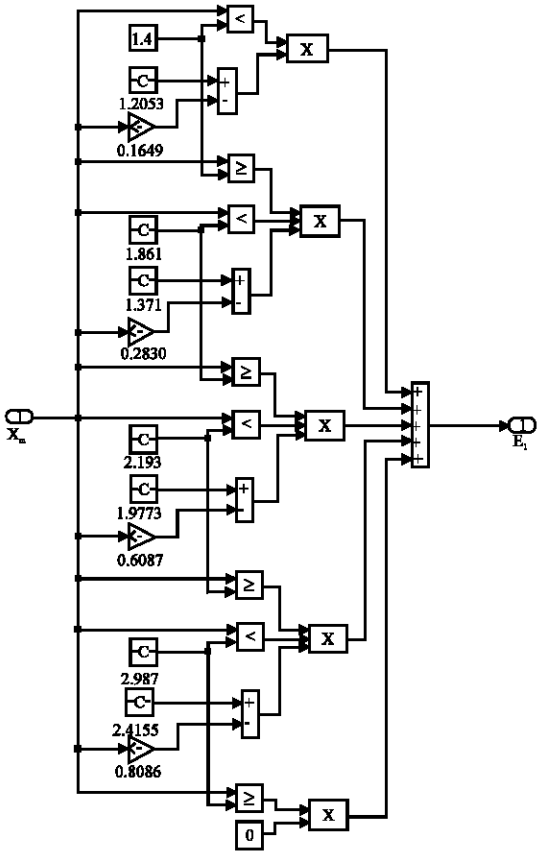

Fig. 9: The subsystem air gap voltage

The subsystem, per unit frequency: Figure 12 consists of several subsystems. These are the subsystems k_2, k_1, k_0 and frequency equation. The details of these subsystems are shown in Fig. 13-16, respectively. They represent Eq. 22-25, respectively.

RESULTS

Several results were obtained from the constructed Simulink block diagrams, Fig. 2 and 11 for a SEIG whose parameters are given in the Appendix (Chan, 1994). The pu value of X_c can be obtained in terms of the per unit excitation capacitance, C_{pu} as follows. The base value of the excitation capacitance, C_b can be obtained from:

$$C_b = \frac{1}{(\omega_b Z_b)}$$

Where:

ω_b = Base angular frequency
Z_b = Base impedance

The actual value of the excitation capacitance, C_{actual} can be obtained from:

$$C_{actual} = C_b C_{pu}$$

Thus, the pu value of X_c is given by:

$$X_c = 1/(\omega_b C_{actual} Z_b)$$

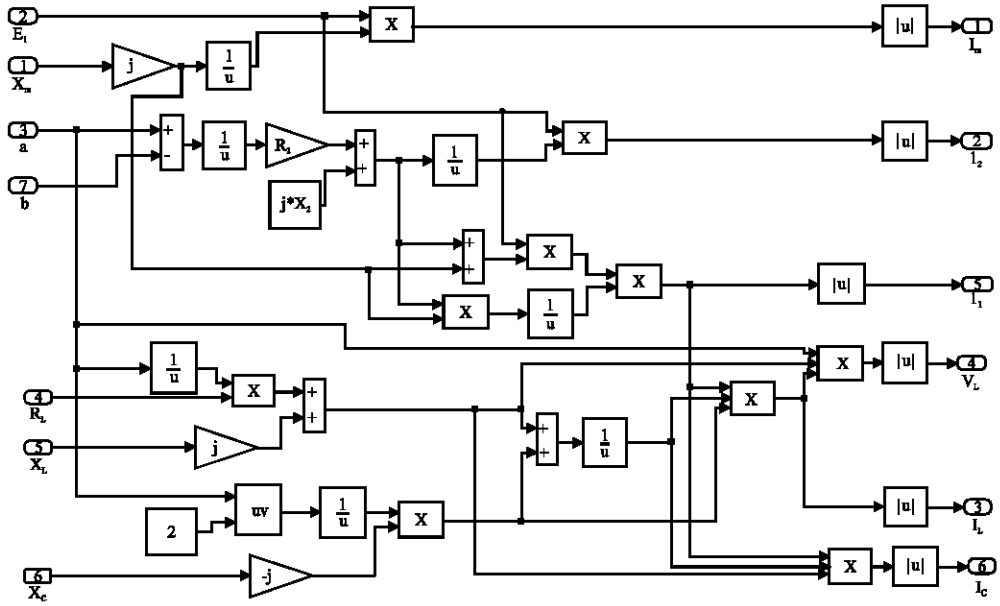

Fig. 10: The subsystem, load voltage and current

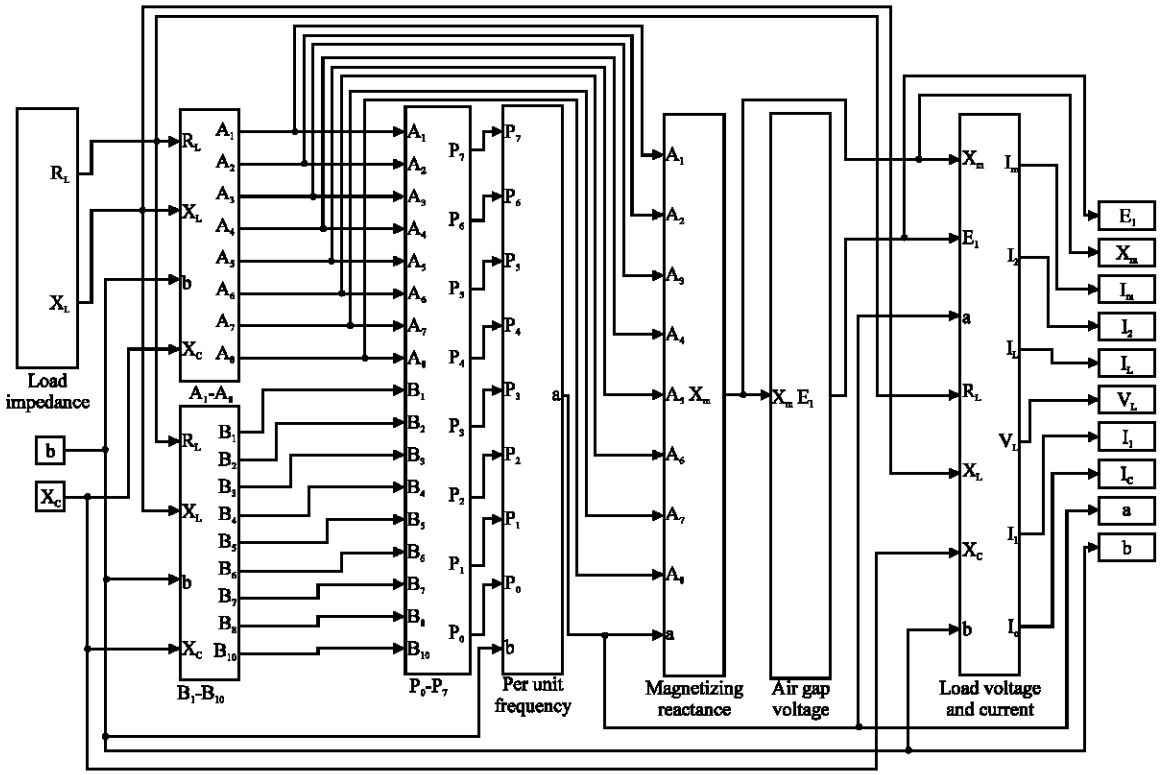

Fig. 11: Simplified overall Simulink block diagram

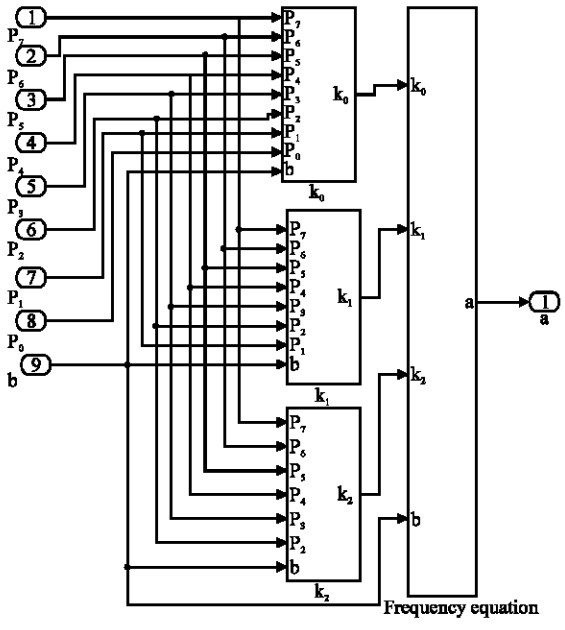

Fig. 12: The simplified subsystem, per unit frequency

Figure 17 shows the relationship between the per unit frequency, a and the load admittance for a load having a 0.8 lagging power factor for two values of the excitation capacitance when the generator is driven at rated speed,

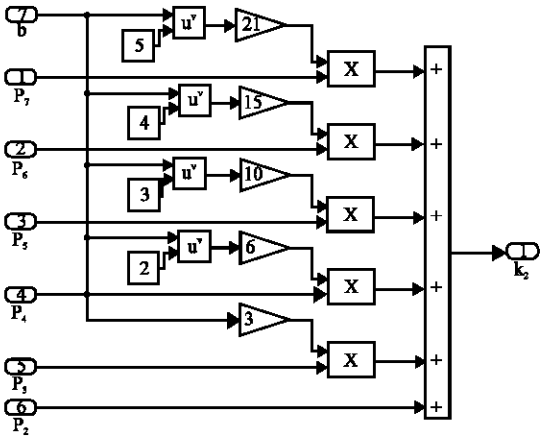

Fig. 13: The subsystem, k_2

b = 1 pu. It can be noticed from this Fig. 17 that the per unit frequency decreases linearly when the load current is increased for certain excitation capacitance. The range of loading the generator is expanded as the excitation capacitance is increased as shown in Fig. 17. It can be noticed also that the results obtained when the simplified method for obtaining the frequency is used are almost identical with the results obtained when the exact method to obtain frequency is used. Figure 18 shows the relationships between magnetizing reactance,

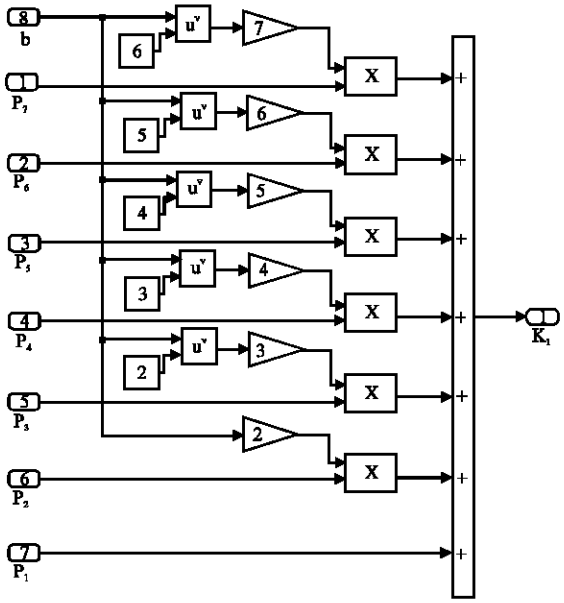

Fig. 14: The subsystem, k_1

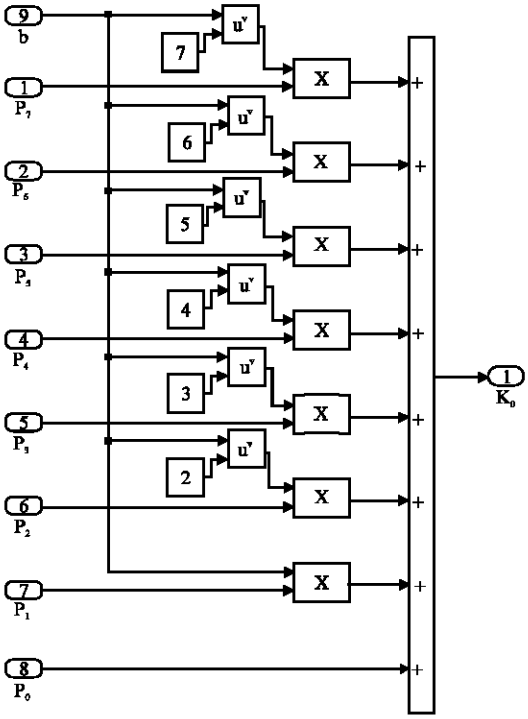

Fig. 15: The subsystem; k_0

X_m with the load admittance, Y_L for two values of the excitation capacitances at 0.8 lagging load power factor and rated generator speed, b = 1 pu. It can be noted that the magnetizing reactance increases in a nonlinear manner with increasing the load current for certain excitation capacitance as shown in Fig. 18.

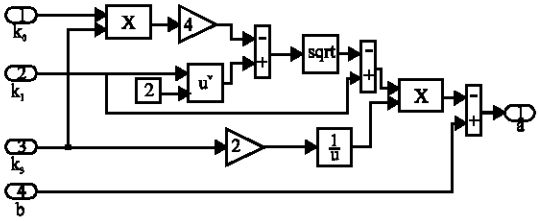

Fig. 16: The subsystem, frequency equation

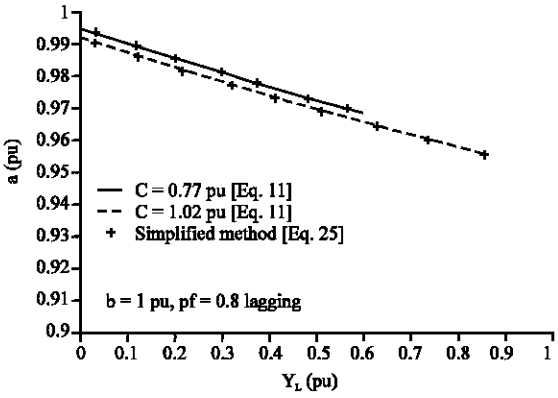

Fig. 17: Variations of the per unit frequency, a with the load admittance, Y_L for two values of the excitation capacitances at 0.8 lagging power factor and rated generator speed

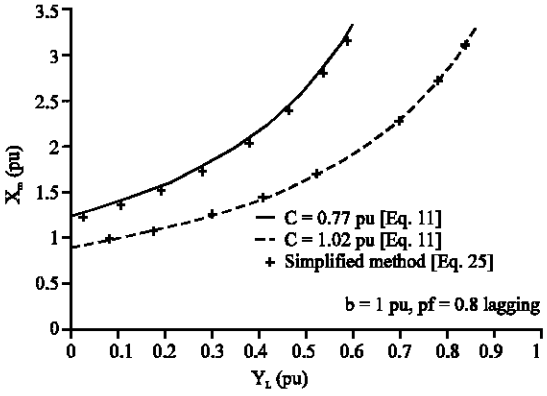

Fig. 18: Variations of the magnetizing reactance, X_m with the load admittance, Y_L for two values of the excitation capacitances at 0.8 lagging power factor and rated generator speed

Figure 19 shows the external characteristics of the SEIG when it is driven at rated speed and is loaded with unity power factor load. The characteristic is drawn using the exact and the simplified methods to obtain the frequency and compared to experimental results obtained from reference (Chan, 1994) for two values of excitation capacitance in order to show its effect on the external

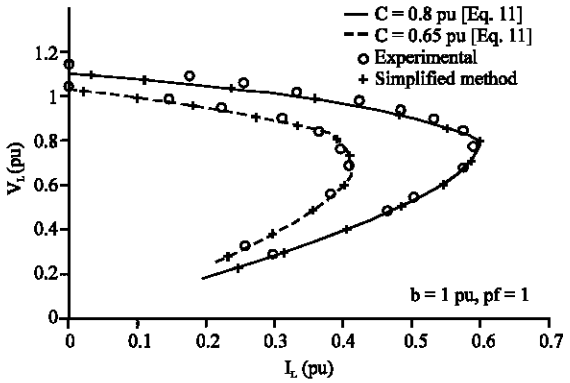

Fig. 19: External characteristics of the SEIG at unity power factor and rated generator speed

characteristics. It can be noticed that the obtained characteristics are approximately identical to those obtained by Chan (1994) which proves the validity of the simulation process.

It can be noticed also that when the excitation capacitance is increased from 0.65-0.8 pu, the voltage regulation is improved and the operating range is expanded. In other words, it increases the operating current capability of the generator.

CONCLUSION

Complete Matlab/Simulink block diagrams are constructed to simulate the SEIG feeding static inductive loads, using the loop impedance method with the frequency obtained using exact and simplified methods. The obtained characteristics using the two methods are compared with each other and found to be almost identical.

The obtained results are also compared to previously experimental results published and the two sets of results were found to be in very close agreement.

APPENDIX

Coefficients A_{1-8}:

$$A_1 = R_L(X_1 + X_2) + X_L(R_1 + R_2)$$
$$A_2 = R_L X_1 X_2 + X_L(R_2 X_1 + R_1 X_2)$$
$$A_3 = b(A_1 - X_L R_2)$$
$$A_4 = bX_2(R_1 X_L + X_1 R_L)$$
$$A_5 = X_c(R_L + R_1 + R_2)$$
$$A_6 = X_c[R_2(X_L + X_1) + X_2(R_L + R_1)] + R_1 R_2 R_L$$
$$A_7 = bX_c(R_L + R_1)$$
$$A_8 = X_2 A_7$$

Coefficients B_{1-10}:

$$B_1 = X_L(X_1 + X_2)$$
$$B_2 = X_1 X_2 X_L$$
$$B_3 = bB_1$$
$$B_4 = bB_2$$
$$B_5 = X_c(X_1 + X_2 + X_L) + R_L(R_1 + R_2)$$
$$B_6 = X_c X_2(X_L + X_1) + R_L(R_1 X_2 + R_2 X_1) + R_1 R_2 X_L$$
$$B_7 = b(B_5 - R_2 R_L)$$
$$B_8 = b[B_6 - R_2(R_1 X_L + X_1 R_L)]$$
$$B_{10} = X_c R_2(R_L + R_1)$$

Coefficients P_{0-7}:

$$P_7 = -A_1 B_2 + A_2 B_1$$
$$P_6 = A_1 B_4 - A_2 B_3 + A_3 B_2 - A_4 B_1$$
$$P_5 = A_1 B_6 - A_2 B_5 - A_3 B_4 + A_4 B_3 + A_5 B_2 - A_6 B_1$$
$$P_4 = -A_1 B_8 + A_2 B_7 - A_3 B_6 + A_4 B_5 - A_5 B_4 + A_6 B_3 - A_7 B_2 + A_8 B_1$$
$$P_3 = -A_1 B_{10} + A_3 B_8 - A_4 B_7 - A_5 B_6 + A_6 B_5 + A_7 B_4 - A_8 B_3$$
$$P_2 = A_3 B_{10} + A_5 B_8 - A_6 B_7 + A_7 B_6 - A_8 B_5$$
$$P_1 = A_5 B_{10} - A_7 B_8 + A_8 B_7$$
$$P_0 = -A_7 B_{10}$$

Induction generator parameters and magnetization curve: Three phase, 4 pole, 50 Hz, 380 V, 5.4 A, 2 kW, star-connected squirrel cage induction machine whose per phase equivalent circuit parameters in per unit are $R_1 = 0.982$, $X_1 = 0.112$, $R_2 = 0.0621$, $X_2 = 0.0952$. The magnetization curve is piecewise linearzed, using the following equations:

$$E_1 = \begin{cases} 1.2053 - 0.1649X_m & X_m < 1.4 \\ 1.371 - 0.2830X_m & 1.4 \le X_m < 1.861 \\ 1.9773 - 0.6087X_m & 1.861 \le X_m < 2.193 \\ 2.4155 - 0.8086X_m & 2.193 \le X_m < 2.987 \\ 0 & 2.987 \le X_m \end{cases}$$

REFERENCES

Abdel-Halim, I.A.M., M.A. Al-Ahmar and M.Z. El-Sherif, 1999. A novel approach for the analysis of self-excited induction generators. Electric Mach. Power Syst., 27: 879-888.

Baroudi, J.A., V. Dinavahi and A.M. Knight, 2007. A review of power converter topologies for wind generators. Renewable Energy, 32: 2369-2385.

Chan, T.F., 1994. Steady-state analysis of self-excited induction generators. IEEE Trans. Energy Conversion, 9: 288-296.

Nesba, A., R. Ibtiouen and O. Touhami, 2006. Dynamic performances of self-excited induction generator feeding different static loads. Serbian J. Electr. Eng., 3: 63-76.

Seyoum, D., C. Grantham and M.F. Rahman, 2003. The dynamic characteristics of an isolated self-excited induction generator driven by a wind turbine. IEEE Trans. Industry Appl., 39: 936-944.

Wang, L. and J.Y. Su, 1999. Dynamic performances of an isolated self-excited induction generator under various loading conditions. IEEE Trans. Energy Conversion, 14: 93-100.